

**SOFIA FORCAST FAR-IR PHOTOMETRY OF COMET ISON AND CONSTRAINTS ON THE COMA GRAIN SIZE DISTRIBUTION.** D. H. Wooden<sup>1</sup>, J. M. De Buizer<sup>2</sup>, M. S. Kelley<sup>3</sup>, C. E. Woodward<sup>4</sup>, D. E. Harker<sup>5</sup>, W. T. Reach<sup>2</sup>, M. L. Sitko<sup>6</sup>, R. W. Russell<sup>7</sup>, R. D. Gehrz<sup>4</sup>, Imke de Pater<sup>8</sup>, Ludmilla Kolokolova<sup>3</sup>

<sup>1</sup>NASA Ames Research Center, Moffett Field, CA 94035, <sup>2</sup>SOFIA, USRA, <sup>3</sup>University of Maryland, College Park, MD, <sup>4</sup>MN Institute of Astrophysics, University of Minnesota, Minneapolis, MN, <sup>5</sup>CASS/UCSD, San Diego, CA, <sup>6</sup>Space Science Institute, Cincinnati, OH, <sup>7</sup>The Aerospace Corporation, El Segundo, CA, <sup>8</sup>University of California Berkeley, Berkeley, CA

**Introduction:** Comet C/2012 S1 (ISON) was unique in that it was a dynamically new comet derived from the nearly isotropic Oort cloud reservoir of comets with a sun-grazing orbit. Infrared (IR) observations were executed on NASA's Stratospheric Observatory For Infrared Astronomy (SOFIA) by the FORCAST<sup>[1]</sup> instrument on 2013 October 25 UT ( $r_h=1.18$  AU,  $\Delta=1.5$  AU). Photometry was obtained in FORCAST filters centered at 11.1, 19.7, and 31.5  $\mu\text{m}$ . The observations compliment a large world-wide effort to observe and characterize comet ISON.

Comet dust properties, including the dust mineralogy, porosity, and grain size distribution parameters are derived by fitting thermal dust models to IR observations of comets. Presently, the dust properties are well constrained for relatively few long-period Nearly Isotropic Comets (NICs) dynamically from the Oort cloud compared to short-period Ecliptic Comets (ECs) from the scattered disk. Previously studied NICs have dust properties that span a range of small and/or highly porous grains (e.g., C/1995 O1 (Hale-Bopp)<sup>[3,4,5]</sup> and C/2001 Q4 (NEAT)<sup>[6]</sup>) to large and/or compact grains (e.g., C/2007 N4 (Lulin)<sup>[7]</sup> and C/2006 P1 (McNaught)<sup>[8]</sup>). For the sample of NICs, silicate crystalline mass fractions range from  $f_{\text{cryst}} \approx 0.1-0.6$ <sup>[8,9]</sup>, which are benchmarks for radial transport in our protoplanetary disk<sup>[10]</sup>. Comet Hale-Bopp near perihelion revealed very strong silicate features, with a silicate strength of  $>3$  and had crystalline peaks near 16, 19, 23.5, 27.5, 33  $\mu\text{m}$ ,<sup>[11]</sup> which yield a high crystalline fraction of  $f_{\text{cryst}} \approx 0.6$ .<sup>[3]</sup> Furthermore, Hale-Bopp's forsterite features' central wavelength positions, relative intensities, and feature asymmetries can constrain the shapes of the forsterite crystals; the crystal shapes are consistent with high temperature disk condensates and evaporates.<sup>[12]</sup> The grain size distribution parameters as well

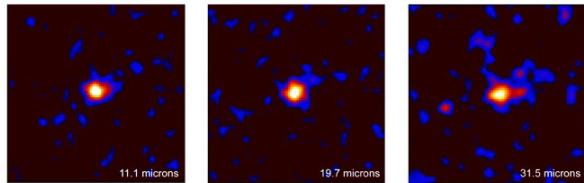


Figure 1. SOFIA FORCAST imaging photometry of comet ISON in 3 filters: 11.1, 19.7, and 31.5  $\mu\text{m}$ .

as the mineralogy give clues to comet origins. In ra-

dial transport models for dust grains in the protoplanetary disk, larger grains ( $\sim 20$   $\mu\text{m}$ ) are harder to transport to larger disk distances ( $> \sim 20$  AU) than smaller grains ( $\sim 1$   $\mu\text{m}$ ).<sup>[13]</sup>

**Dust Modeling Methods:** Through modeling of observations of 10  $\mu\text{m}$  silicate emission feature and its strength,<sup>[2]</sup> the mineralogy can be constrained. For observations with sufficient signal-to-noise ratio (SNR), models can constrain the silicate-to-carbon ratio and the olivine-to-pyroxene ratio. If a 11.1–11.2  $\mu\text{m}$  peak from forsterite is detected, then the models further constrain the silicate crystalline-to-amorphous ratio, or crystalline fraction  $f_{\text{cryst}} = m_{\text{cryst}} / (m_{\text{amor}} + m_{\text{cryst}})$ . Through modeling the mid- and far-IR flux densities, we constrain the properties of the grain size distribution (GSD) and grain porosity ( $P$  versus dust radius  $a$ , parameterized by  $D$  such that  $P = (a/0.1 \mu\text{m})^{(D-3)}$ ,  $D=3$  for solid and  $D=2.5$  for highly porous).<sup>[7]</sup> In a Hanner (modified power-law) grain size distribution,<sup>[7]</sup> the small radii grains at the peak of the grain size distribution ( $a_p$ ) dominate the surface area and the flux density. Smaller grains produce higher contrast silicate features. Grains of greater porosity grains also produce higher contrast silicate features. Similarly, larger grains are cooler, contribute to the ‘continuum’ under the silicate feature and contribute to the far-IR flux density. A steeper grain size distribution has more smaller grains relative to larger grains, so a steeper grain size distribution can produce a stronger silicate feature because the smallest grains dominate the dust emitting surface area. More smaller grains also can produce a stronger  $\sim 3.5-8$   $\mu\text{m}$  ‘featureless’ continuum, which is typically attributed to submicron amorphous carbon grains.<sup>[2,8,9,10,14]</sup> The amorphous carbon featureless emission extends through the 10  $\mu\text{m}$  region, so a higher amorphous carbon-to-silicate ratio also can weaken the silicate feature.<sup>[6]</sup> As described by these examples, the mineralogy and grain size distribution parameters (porosity,  $a_p$ , and slope  $N$ ) are coupled and must be sought simultaneously when fitting thermal models to comet IR observations. Even with these modeling complexities, given measurements of the silicate feature strength, the color temperature of the 10  $\mu\text{m}$  continuum, and three photometry measurements near 11.1, 19.7, and 31.5  $\mu\text{m}$ , this is sufficient informa-

tion to constrain the silicate-to-carbon ratio and grain size distribution parameters (porosity,  $a_p$ , and slope  $N$ ).

### Dust Models of Comet ISON ( $r_h \approx 1.2$ AU):

For modeling comet ISON at this epoch, we consider three mineral compositions: amorphous carbon, and amorphous silicates with 50% olivine and 50% pyroxene. We consider a grain size distribution (GSD) spanning grain radii  $0.1 \leq a \leq 1000 \mu\text{m}$ , slopes  $3.2 \leq N \leq 4.5$  in steps of 0.1, and four porosities characterized by porosity parameter<sup>[7]</sup>  $D=2.500, 2.727, 2.857,$  and  $3.000$ . When the thermal models are fitted to the FORCAST photometry points and employ the constraint on the silicate feature strength ( $\leq 1.1$ ) given from ground-based N-band spectra by T. Ootsubo and collaborators,<sup>[15]</sup> then lower reduced goodness-of-fit ( $\chi_v^2$ ) values are achieved for smaller  $a_p$  and steeper slopes  $N$ , as shown in the four-panel Fig. 2. If the constraint of color temperature of the N-band continuum is added to the thermal model fits, then low  $\chi_v^2$  values are achieved for larger  $a_p$  ( $0.7 \mu\text{m} \leq a_p \leq 1.0 \mu\text{m}$ ), porosity parameter  $P=2.7$ , and an even steeper GSD slope ( $N=4.5$ ), as shown in Fig. 3. The N-band color temperature is an important constraint on the GSD.

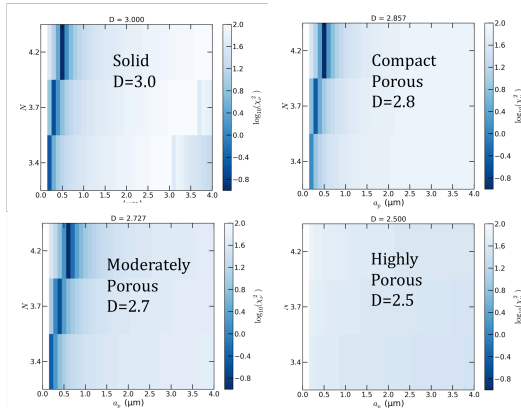


Figure 2: Reduced  $\chi_v^2$  for thermal models fitted to three FORCAST photometry points and with the constraint that the silicate feature strength  $\leq 1.1$  for comet ISON at  $r_h \approx 1.2$  AU.

**Results:** Thermal model fits to SOFIA +FORCAST broadband photometry of comet ISON at three wavelengths, 11.1, 19.7 and 31.5  $\mu\text{m}$ , offer constraints on the coma grain size distribution when combined with a limit on the silicate feature strength ( $\leq 1.1$ ) and color temperature (260–265 K) of the continuum on the short and long wavelength sides the silicate feature, as measured within a week of FORCAST photometry by Subaru COMICS ground-based N-band spectroscopy.<sup>[15]</sup> For this epoch ( $r_h \approx 1.2$  AU), comet ISON is better fitted by thermal models with dust properties including moderately porous grains ( $D=2.7$ ), a peak grain radius of  $0.7 \mu\text{m} \leq a_p \leq 1 \mu\text{m}$ , and a size distribu-

tion slope of  $N=4.5$ . The peak grain radius of comet ISON at this epoch is more similar to two Oort clouds comets with large/and or compact porous grains (C/2007 N4 (Lulin)<sup>[7]</sup> and C/2006 P1 (McNaught)<sup>[8]</sup>), but its size distribution slope is considerably steeper than all other NICs. For such a steep grain size distribution to generate such a weak silicate feature requires little silicates compared to carbon. Specifically, amorphous carbon : silicate  $\approx 0.9 : 0.1$ . At this epoch, comet ISON's amorphous carbon-to-silicate ratio is high compared to other NICs from the Oort cloud and is on the high end of the range of all comets including Ecliptic Comets from the scattered disk<sup>[8]</sup>. Comet ISON's thermal emission is dominated by  $\sim 0.7\text{--}1 \mu\text{m}$  grains that are carbon rich.

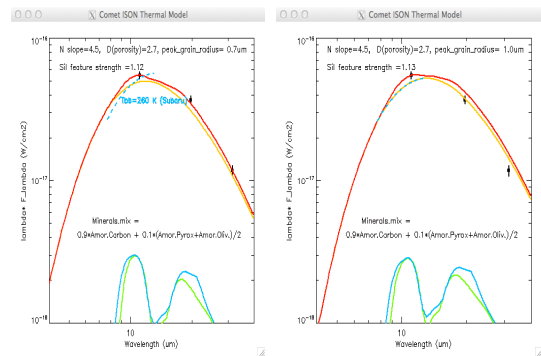


Figure 3: Better-fit thermal models for comet ISON at  $r_h \approx 1.2$  AU, for  $a_p = 0.7 \mu\text{m}$  (left) and  $a_p = 1.0 \mu\text{m}$  (right), porosity parameter  $D=2.7$  and slope  $N=4.5$ . Models are fitted to three FORCAST photometry points (black points with error bars, and constrained by the silicate feature strength  $\leq 1.1$  and the N-band continuum color temperature of  $T_{bb} = 260\text{--}265 \text{ K}$ <sup>[15]</sup> (blue dashed line of a graybody at this temperature). Mineralogy is amorphous carbon-to-amorphous silicate ratio = 9, with amorphous carbon (orange), amorphous pyroxene, amorphous olivine (green), and the total SED (red).

### References:

- [1] Adams, J.D., et al. 2012, *SPIE*, 8446, 16
- [2] Kelley, M.S., Wooden, D.H. 2009, *PSS*, 57, 1133
- [3] Harker et al. 2002, *ApJ*, 580, 579;
- [4] Hayward et al. 2000, *ApJ*, 538, 428
- [5] Hadamcik, E., Levasseur-Regourd, A.C. 2003, *JQSRT*, 79–80, 661
- [6] Wooden, D.H. 2004, *ApJL*, 612, L77
- [7] Woodward et al. 2011, *AJ*, 141, 181
- [8] Kelley et al. 2010, *LPSC*, 41, #2375
- [9] Kelley, M.S. et al. 2011, *AAS*, 211, 560
- [10] Wooden, D.H. 2008, *SSRv*, 138, 75
- [11] Crovisier, J. et al. 1997, *Science* 275, 1904
- [12] Lindsay, S.S. et al. 2013, *ApJ*, 766, 54
- [13] Hughes, A.H., Armitage, P.J. 2010, *ApJ*, 719, 1633
- [14] Hanner, M.S., Zolensky, 2010, *Astromineralogy, Lecture Notes in Phys.*, Vol. 815, 203
- [15] Ootsubo, T. et al. 2013, AGU 2014 Fall Meeting, #P24A-06